Nonlinear Geometric Temperature Control of a Vinyl Acetate Emulsion Polymerization Reactor

ARTICLE *in* INDUSTRIAL & ENGINEERING CHEMISTRY RESEARCH · DECEMBER 2013

Impact Factor: 2.59 · DOI: 10.1021/ie402296j

3 AUTHORS:

Ivan Gil

National University of Colombia

35 PUBLICATIONS **169** CITATIONS

SEE PROFILE

Julio Cesar Vargas

National University of Colombia

20 PUBLICATIONS **284** CITATIONS

SEE PROFILE

Jean-Pierre Corriou

University of Lorraine

130 PUBLICATIONS **1,275** CITATIONS

SEE PROFILE

I&EC research
Industrial & Engineering Chemistry Research

Article

pubs.acs.org/IECR

Nonlinear Geometric Temperature Control of a Vinyl Acetate Emulsion Polymerization Reactor

Iván D. Gil,[†,‡] Julio C. Vargas,[†] and Jean P. Corriou*[,‡]

[†]Departamento de Ingeniería Química y Ambiental, Universidad Nacional de Colombia, Bogotá, Cundinamarca 111321, Colombia
[‡]Laboratoire Réactions et Génie des Procédés, CNRS, Université de Lorraine, ENSIC 1, Rue Grandville, B.P. 20451, 54001, Nancy Cedex, France

Supporting Information

ABSTRACT: In this paper, an industrial emulsion polymerization process, which is characterized by exothermic reactions with complex nonlinear dynamics, is addressed. In this process vinyl acetate is used as monomer, potassium persulfate as initiator and polyvinyl alcohol as protective colloid. A model of the system to calculate average molecular weight and dispersity is implemented. A fine and strict temperature control is required in order to guarantee the product quality and safe operation. Nonlinear geometric control based on input/output linearization is used for reactor temperature control. An extended Kalman filter is implemented to estimate unmeasured states. Performance tests of the controller and state estimator are carried out by introducing modeling and estimator errors. It is also verified that the nonlinear controller can work with different initiator feed policies helping to improve the process productivity. Finally, compared to a traditional PID controller, the nonlinear geometric controller is superior in rejecting disturbances and performing set point tracking.

1. INTRODUCTION

Emulsion polymerization is a process employed to convert a variety of unsaturated organic compounds into large chains through radical chain polymerization. In this type of polymerization, the monomers polymerize in the form of emulsions (i.e., colloidal dispersions) using an inert medium in which the monomer is moderately soluble (not totally insoluble).[1,2] Commercial polymerizations of vinyl acetate, chloroprene, various acrylate copolymers, and copolymerizations of butadiene with styrene are carried out by emulsion polymerizations. Compared to other types of polymerization, emulsion processes present important advantages mainly related to the physical state of the emulsion which facilitates the reaction control. For example, viscosity and heat transfer problems are less significant than in bulk polymerization. The product of an emulsion polymerization can be used directly without additional separation steps.[1] Some common applications include paints, coatings, finishes and floor polishes. The demand for new latex products has increased rapidly together with the research efforts in modeling, optimization and control of emulsion polymerization processes. The growth in this area was limited by the understanding of the chemistry and physics of these systems. However, nowadays, the level of knowledge has improved importantly inducing an increased complexity of the models. This complexity arises from factors such as their multiphase nature, nonlinear behavior and sensitivity to disturbances.[3,4] One of the goals in building a model is to use it to optimize productivity or to control some quality product specifications, such as molecular weight, long chain branching and cross-linking frequency, particle morphology, viscosity, solids content, particle size distribution, and gel contents, among others.[3] In particular, this work proposes to perform an efficient control of reactor temperature, one of the main variables which influences the reaction behavior and thus the final polymer properties.

Control of polymerization reactors is a challenging task because of the complexity of the physicochemical phenomena and the polymerization reaction kinetics, in addition to the difficulties related to the availability of hardware sensors to provide online measurement of the end-use polymer properties. Normally, polymer properties are related to the molecular weight distribution (MWD), particle size distribution (PSD), glass transition temperature, morphology, and composition (in the case of copolymerization and terpolymerization reactions), among others.[5−8] As many other processes, emulsion polymerization must be operated under safe conditions while achieving the characteristics of the products in terms of quality and production rate. The trend in industrial operation is to use a polymerization reactor to manufacture a variety of products at different grades involving frequent startups, transitions, and shutdowns[6] that demand the design of effective process control and monitoring strategies. Polymerization reactors are some of the processes in which many process variables related to end-use properties or product quality can only be measured at low sampling rates, with frequent time delays[9] or even measured off-line. For this reason, in polymerization processes, it is interesting to develop state estimators capable of estimating unmeasurable properties from other available measurements. The development of reliable state estimators is subjected to the availability of sufficiently accurate, based on first principles, mathematical models of the phenomena involved.[10,11] Moreover, another advantage of state observers is the possibility of

Special Issue: John Congalidis Memorial

Received: July 18, 2013
Revised: December 16, 2013
Accepted: December 18, 2013
Published: December 19, 2013

dx.doi.org/10.1021/ie402296j | Ind. Eng. Chem. Res. 2014, 53, 7397−7408

reducing the influence of measurement noise and modeling uncertainties, allowing their application in process monitoring, control, fault detection, and as filters of random effects associated with the measurements.[8] In particular, control of emulsion polymerization to produce polyvinyl acetate has been reported recently[12,13] by means of PID techniques to control the temperature in the reactor trying to reduce variability in the system and to increase productivity at the same time. Arora et al.[12] use monomer flow rate as the manipulated variable to control the temperature influencing the reaction rate directly. In this case where evaporative cooling is coupled with jacket cooling to remove the reaction heat, the largest part of the generated heat is removed by the jacket and additional control loops for pressure and water concentration in the gas phase are required in the operation. However, in the cases where PID control is used and the cooling capacity of the reactor is limited with respect to the reaction heat, as in Hvala et al.,[13] where there is no jacket for the reactor, the temperature range is very limited and oscillations can affect polymer quality as a consequence of the dynamics of the recycle stream from the condenser, which generates multiple steady states, among others. Wang et al.[14] already studied in simulation nonlinear control, in an adaptive framework, of batch styrene polymerization. Sheibat−Othman and Othman[15] reported the use of online nonlinear geometric control of a laboratory emulsion polymerization reactor where reactor temperature and remaining moles of monomer in the reactor were the controlled variables. Nonlinear geometric control of an industrial gas phase copolymerization reactor has been also studied by Corriou[16] using states estimated by means of extended Kalman filtering or predicted from the kinetic process model.[16,17] In these studies, it is demonstrated that nonlinear geometric control is suitable for disturbance temperature rejection in a highly exothermic reaction.

In the present work, nonlinear geometric control is used in simulation to track the temperature of an industrial emulsion polymerization reactor around a desired trajectory by adjusting the inlet jacket temperature. An extended Kalman filter is proposed to estimate the states of a reduced model that are used in the control law calculations. The results show that nonlinear control offers a good performance in controlling nonlinear processes such as emulsion polymerization and also allows us to explore new operating strategies to improve reactor performance and quality parameters of the polymer.

2. PROCESS DESCRIPTION

An emulsion polymerization process displays different behaviors according to the relative rates of initiation, propagation, and termination, which at the same time depend on the monomer and reaction conditions. The process in which the polymer particles are nucleated and then grow in size is divided into three intervals which are based on the particle number N and the existence of a separate monomer phase (i.e., monomer droplets), which exists in the intervals I and II but not in III.

In a real plant, initially, specific quantities of monomer, initiator, water, and protective colloid are charged to the reactor according to a recipe. In the process studied here, according to the procedure followed in a Colombian small chemical plant, vinyl acetate is used as monomer, potassium persulfate as initiator and polyvinyl alcohol as protective colloid. A preheating step of the reactor is carried out by injecting steam or hot water into the reactor jacket in order to reach a temperature of 350 K. The reactor must be maintained at this temperature to ensure complete dissolution of the polyvinyl alcohol. The reaction starts when the activation temperature of the initiator is reached (approximately 345 K). The remaining monomer, according to the recipe, is fed continuously during the major part of the batch whereas the initiator is injected by finite impulses at two or three different instants during the batch. The agitation speed is constant. The initiator and monomer temperature correspond to the external temperature. Because of the exothermicity of the reaction, high quantities of heat are released and temperature inside the reactor is controlled around a constant value by adjusting the jacket temperature. Three main input variables to the process can be identified, monomer flow rate, initiator flow rate and inlet jacket temperature which is adjusted by means of a three way valve. Temperature is considered as an output measured variable. Figure 1 shows the schematic industrial reactor configuration.

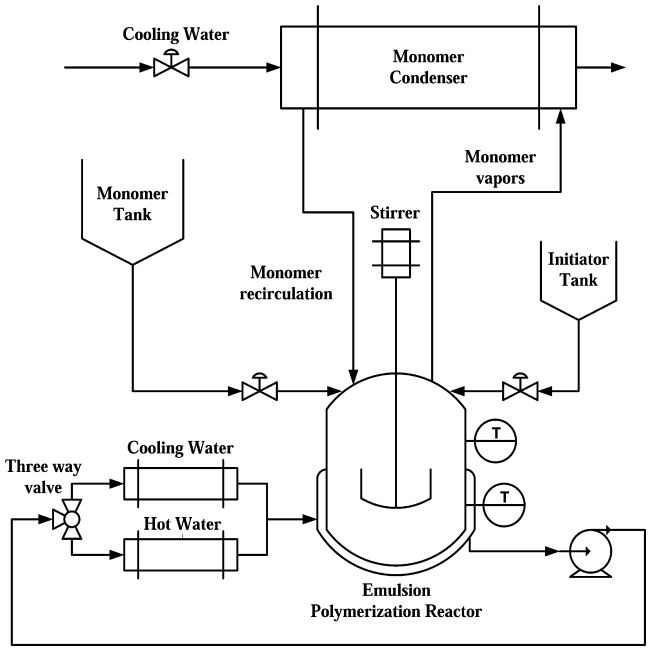

Figure 1. Process flow diagram for emulsion polymerization.

3. PROCESS MODEL

A model based on the leading moments of the molecular weight distribution (MWD) is used to represent the state of the polymer. Although the emulsion polymerization takes place in three different liquid phases (monomer or droplet phase, water or aqueous phase, and the particle phase), the reaction is mainly carried out in the particle phase. The main assumptions used in the development of this model are based on the work of Arora et al., 2007: (1) The values of the kinetic rate constants in the polymer and aqueous phases are equal. (2) The kinetic rate constants do not depend on chain length. (3) For radicals, the pseudo-steady state is assumed. (4) The number of particles N_p is constant (e.g., by the usage of seed). (5) The reactivities of radicals generated by initiation or chain transfer are similar.

Vinyl monomers, such as vinyl acetate and acrylate esters, polymerize only by addition processes. These kinds of processes differ according to the type of initiator used which induces free radical, ionic, or high energy mechanisms. However, all these mechanisms are similar, including initiation, propagation and termination steps.[2,18] In the initiation step, the initiator (I) dissociates to yield a pair of free radicals ($R^{\bullet}$) and

dx.doi.org/10.1021/ie402296j | Ind. Eng. Chem. Res. 2014, 53, 7397−7408

then the addition of the free radical to the first monomer (M) molecule having a vinyl double bond to produce chain-initiating species (R_1)

$$I \xrightarrow{k_d} 2R^{\bullet} \tag{1}$$

$$R^{\bullet} + M \xrightarrow{k_i} R_1 \tag{2}$$

The dissociation of the initiator is the rate-determining step in the initiation sequence. In a second stage, the process of the growth of (R_1) by the successive addition of a large number of molecules (n) is known as propagation. In this step, the monomer molecules are converted to polymer from the initial radical species produced in the first step

$$R_n + M \xrightarrow{k_p} R_{n+1} \tag{3}$$

where k_p is the rate constant for propagation.

Chain transfer to monomer (eq 4) and to polymer (eq 5) reactions are responsible for the formation of radicals R_1 and R_m, and the polymer chain P_n

$$R_n + M \xrightarrow{k_{fm}} P_n + R_1 \tag{4}$$

$$R_n + P_m \xrightarrow{k_{fp}} P_n + R_m \tag{5}$$

where k_{fm} and k_{fp} are the rate constants for chain transfer to monomer and chain transfer to polymer, respectively.

The termination is the final mechanism used to stop the propagating polymer chain in some specified conditions of conversion, solids content, molecular weight, among others. Two mechanisms of termination are reported: (1) Biradical coupling

$$R_n + R_m \xrightarrow{k_{tc}} P_{n+m} \tag{6}$$

in which two polymeric radicals terminate each other by the occurrence of the elimination of the radical centers. (2) Disproportionation

$$R_n + R_m \xrightarrow{k_{td}} P_n + P_m \tag{7}$$

in which one polymeric radical subtracts a hydrogen atom from another polymeric radical, leaving it with a terminal vinyl double bond. As a result, two polymer molecules are formed, one saturated and one unsaturated.

3.1. Initiator Balance. The first mole balance equation corresponds to the initiator

$$\frac{dI}{dt} = q_I - k_I I \tag{8}$$

where q_I is the flow rate of initiator fed to the reactor and k_I is the overall initiation rate constant which takes into account the combined effect of the decomposition and consumption rate constants.

3.2. Monomer Balance. The total amount of monomer added to the reactor is described by

$$\frac{dM_t}{dt} = q_M \tag{9}$$

where q_M is the flow rate of monomer fed to the reactor during the batch. The amount of monomer remaining M_M in the reactor increases because of the monomer feed flow rate and decreases because of the polymerization reaction $\mathcal{R}_{pol}$

$$\frac{dM_M}{dt} = q_M - \mathcal{R}_{pol} \tag{10}$$

The overall reaction rate of monomer is the sum of the propagation reaction rates in the aqueous phase $\mathcal{R}^w_{pol}$ and in the polymer phase $\mathcal{R}^p_{pol}$

$$\mathcal{R}_{pol} = \mathcal{R}^p_{pol} + \mathcal{R}^w_{pol} \tag{11}$$

Normally, the propagation rate in the polymer phase is much larger than the propagation rate in the aqueous phase. For this reason, it is often neglected for simplification. However, it is important to remember that, when the nucleation phenomena have an important effect, especially the homogeneous nucleation, the propagation rate in the aqueous phase plays an important role in the total calculation of the overall reaction rate.

The polymerization rate in the particle phase can be written as

$$\mathcal{R}^p_{pol} = \frac{k_p \bar{n} N_p [M]^p}{N_{iA}} \tag{12}$$

where $\bar{n}$ denotes the average number of radicals per particle, N_p the total number of particles, and N_A Avogadro's number. Here, N_p is considered constant because the emulsion polymerization seed is part of the initial conditions. The monomer concentration in the particle phase $[M]^p$ is calculated from the phase distribution equations. The polymerization rate in the aqueous phase is influenced by the solubility of the monomer in water. For example, in the case of styrene, which is highly insoluble, the propagation rate in the aqueous phase can be neglected compared to the propagation rate in the polymer phase. However, in the case of vinyl acetate which it is moderately soluble, the effect of the propagation rate in the water phase must be considered. It can be written as

$$\mathcal{R}^w_{pol} = k_p [R]^w V^w [M]^w \tag{13}$$

where k_p is the propagation rate coefficient and $[R]^w$ the overall concentration of radicals in the water phase. $[M]^w$ represents the concentration of monomer in the water phase, which is also obtained from the solution of the phase distribution equations.

3.3. Average Number of Radicals Per Particle $\bar{n}$. Many approaches can be used for the modeling of the average number of radicals per particle.[19−23] One of the first proposals for complete solution of $\bar{n}$ for all intervals is made by Li and Brooks[24] in a simple way

$$\bar{n} = \frac{2\sigma}{k + q} \tag{14}$$

where σ is the average rate of radical entry into a single particle, k is the rate coefficient for radical exit from particle, and q is a parameter.

3.4. Radicals in the Aqueous Phase. Initially, the mole balance used to calculate the number of radicals in the aqueous phase can be written as

$$\frac{d[R]^w}{dt} = 2fk_I[I] + \frac{k\bar{n}N_p}{N_A V^w} - \frac{k_a [R]^w N_p}{N_A V^w} - k_t^w ([R]^w)^2 \tag{15}$$

where the left-hand side is considered null according to the assumption of pseudo-steady state. In consequence, the differential equation is converted to an algebraic equation. In the right-hand side of the radical balance (eq 15), the first term represents the rate of generation of radicals, the second term the rate of desorption from the particles, the third term the rate

dx.doi.org/10.1021/ie402296j | Ind. Eng. Chem. Res. 2014, 53, 7397−7408

of absorption of radicals from the aqueous phase to the particle phase and the fourth term the rate of termination of radicals in the aqueous phase.

3.5. Monomer Phase Distribution. In the same way as the monomer balance equation (eq 10), the volume balance equation is expressed as

$$\frac{dV_{pol}^{p}}{dt} = \mathcal{R}_{pol}\frac{M_{wM}}{\rho_{pol}} \tag{16}$$

where V_{pol} is the total volume of polymer generated in the reaction. After the calculation of V_{pol}, the phase distribution calculations can be performed. The monomer distribution in the aqueous phase, droplet phase and polymer phase uses a method of constant partition coefficients based on three main assumptions: (1) the monomer is in thermodynamic equilibrium between the three phases, (2) the partition coefficients are constant, and (3) the quantity of water in the droplet and in the polymer phase is negligible. The equations of the monomer phase distribution are written as

$$V_M^p + V_M^d + V_M^w = V_M \tag{17}$$

$$V_M^p + V_{pol}^p = V^p \tag{18}$$

$$V_M^w + V_W^w = V^w \tag{19}$$

where the superscripts d, p, and w denote the droplet, particle and aqueous phases, respectively, and subscripts M, W, and pol denote the species. The partition coefficients can be calculated as

$$\frac{V_M^p/V^p}{V_M^w/V^w} = K_M^p \tag{20}$$

$$\frac{V_M^d/V^d}{V_M^w/V^w} = K_M^d \tag{21}$$

In this case, there is only one monomer in the droplet phase leading to the following equation

$$V_M^d = V^d \tag{22}$$

3.6. Moments of Dead Chains. The moments of dead chains of polymer are calculated from eqs 23 to 25[12]

$$\frac{d\mu_0}{dt} = (k_{fm}[M]^p + k_{fp}\mu_0 + k_t\lambda_0)\alpha\lambda_0 - k_{fp}\lambda_0(\mu_0 - (1-\alpha)^2\alpha\lambda_0) + 0.5k_t{\lambda_0}^2 \tag{23}$$

$$\frac{d\mu_1}{dt} = \frac{\lambda_0}{1-\alpha}((k_{fm}[M]^p + k_{fp}\mu_0 + k_t\lambda_0)\alpha(2-\alpha) + k_t\lambda_0) - k_{fp}{\lambda_0}^2(1-\alpha(1-\alpha)^2) \tag{24}$$

$$\frac{d\mu_2}{dt} = \frac{\lambda_0}{(1-\alpha)^2}(2\alpha(k_{fm}[M]^p + k_{fp}\mu_0 + k_t\mu_0) + k_t\lambda_0(2\alpha+1)) - 2k_{fp}{\lambda_0}^2\left(\frac{1-\alpha(1-\alpha)^3}{1-\alpha}\right) + \frac{d\mu_1}{dt} \tag{25}$$

where α is the probability of propagation and λ_0 the total concentration of zeroth moment for growing chains.

The number average molecular weight $\bar{M}_n$ and the weight average molecular weight $\bar{M}_w$ are calculated using the following equations

$$\bar{M}_n = M_{wM}\frac{\mu_1}{\mu_0} \tag{26}$$

$$\bar{M}_w = M_{wM}\frac{\mu_2}{\mu_1} \tag{27}$$

and the dispersity is

$$D = \frac{\bar{M}_w}{\bar{M}_n} \tag{28}$$

3.7. Energy Balance Equations. The temperature of the reactor contents is controlled by means of a jacket which uses water at a constant and large flow rate. Two heat exchangers (Figure 1), one cold, one hot, are used to adjust the temperature of the heating−cooling fluid $T_{j_{in}}$ at the inlet of the jacket by means of a three way valve. The energy balance for the jacket results as

$$\frac{dT_j}{dt} = \frac{F_j(T_{j_{in}} - T_j)}{m_w} - \frac{UA}{m_w C_{p,water}}(T_j - T) \tag{29}$$

where m_w is the mass of water in the reactor jacket, F_j is the heating−cooling fluid flow rate, and

$$T_{j_{in}} = uT_{hot} + (1-u)T_{cold} \tag{30}$$

where T_{cold} and T_{hot} are the respective temperatures of the two heat exchangers. The value of the position u of the three way valve results from from the control law (eq 46). The algebraic equation (eq 30) is obtained by neglecting the dynamics of the heat exchangers and simplification of their behavior. The control by manipulation of the inlet jacket temperature rather than by manipulation of the flow rate of the heating−cooling fluid is more efficient as it avoids to vary the heating−cooling fluid flow rate and thus does not modify the turbulent heat exchange coefficient.

The energy balance of the reactor contents takes into account the energy exchanged through the heating jacket, the heat released by the exothermic reaction, the reactant feed, the cooling of the reactor by the reflux of the condenser

$$\frac{dT}{dt} = \frac{\sum q_i C_{p,i}(T_i - T) - \Delta H_r \mathcal{R}_{pol} + UA(T_j - T) - Q_{cond}}{\sum m_i C_{p,i}} \tag{31}$$

The condenser heat duty calculation follows the proposition by Hvala et al.,[13] where the cooling water flow rate used in the condenser has been fixed and, in consequence, condenser heat duty is considered constant. The overall heat transfer coefficient is calculated by relating it to the relative solids content of the reacting mixture that changes during the batch as in Sáenz de Buruaga et al.[25] and Vicente et al.,[26] and according to the following expression

$$U = U_o + (U_f - U_o)\phi_S^z \tag{32}$$

Finally, two models are used, a first complete model, which includes initiator and monomer balances (eqs 8−10), radicals balance (eq15), volume balance (eq 16), moment equations (eqs 23−25), and energy balances (eqs 29−31), and a second reduced model in which the three differential equations for the moments of dead chains (eqs 23−25) are not taken into account.

dx.doi.org/10.1021/ie402296j | Ind. Eng. Chem. Res. 2014, 53, 7397−7408

Table 1. Model Parameters

parameter	value	units	ref
k_p	6.14×10^{10} exp $(-6.3 \times 10^3/1.987T)$	$cm^3\ mol^{-1}\ s^{-1}$	Mckenna et al.[27]
k_I	2.6×10^{17} exp $(-3.3 \times 10^4/1.987T)$	s^{-1}	Penlidis[28]
N_A	6.023×10^{23}	mol^{-1}	Hvala et al.[13]
M_{wM}	86.09	g/mol	Yildirim[2]
M_{wPVOH}	205,000	g/mol	Hvala et al.[13]
ρ_M	0.8	g/cm^3	Hvala et al.[13]
ρ_{pol}	1.17	g/cm^3	Hvala et al.[13]
ρ_W	1.0	g/cm^3	Hvala et al.[13]
K_M^p	29.5		Araùjo and Giudici[29]
K_M^d	34.7		Araùjo and Giudici[29]
k_{fm}	$2.43 \times 10^{-4}\ k_p$	$cm^3/mol\ s$	Chatterjee et al.[30]
k_{fp}	$2.36 \times 10^{-4}\ k_p$	$cm^3/mol\ s$	Chatterjee et al.[30]
k_t	4.643×10^9 exp $(-2.8 \times 10^3/1.987T)$	$cm^3/mol\ s$	Mckenna et al.[27]
$C_{p,water}$	4.18	J/g K	Hvala et al.[13]
C_{pM}	1.17	J/g K	Yildirim[2]
$C_{p\ pol}$	1.77	J/g K	Arora et al.[12]
C_{pPVOH}	1.65	J/g K	Hvala et al.[13]
ΔH_r	87500	J/mol	Yildirim[2]
z	3		Vicente et al.[26]
U_o	490	$W/m^2\ K$	Vicente et al.[26]
U_f	250	$W/m^2\ K$	Vicente et al.[26]

4. NONLINEAR GEOMETRIC CONTROL AND STATE ESTIMATION

Industrial scale reactors present heat removal problems associated to large polymerization heats and high viscosities of the latexes that limit the heat transfer and, at the same time, limit the rate of polymerization.[8,25] Highly nonlinear behavior, insufficient and delayed measurements, and unmeasured disturbances result in poor performance and robustness problems when classical linear techniques such as PI and PID controllers are applied. Semibatch emulsion polymerization exhibits a particular nonlinear behavior which motivates us to use nonlinear control techniques. Several difficulties are encountered with online measurements in emulsion polymerization systems, ranging from latex sampling and handling of time delays introduced by long analysis times. In real-life industrial reactors, the measurements of all the major properties of the polymer are unavailable, but probably only a few operational variables such as temperature, sometimes viscosity or density, can be measured in order to monitor and control the operation.[3,4,31] To overcome these problems, a nonlinear state estimator is coupled to nonlinear geometric control technique based on input/output (I/O) linearization to control the reactor temperature. The state estimator allows us to estimate states which can be used to monitor the polymerization process and which are used in the nonlinear control law developed in the state space. Figure 2 shows the principle of nonlinear geometric control coupled with state estimation.

4.1. Nonlinear Geometric Control. Nonlinear geometric control is based on differential geometry and Lie algebra.[17,32−36] The control law design is based on the nonlinear state space model allowing to take into account the system nonlinearities. For that reason, nonlinear geometric control is considered appropriate in highly nonlinear systems like emulsion polymerization. It is necessary to represent the system as an affine model with respect to the manipulated inputs, which is most often the case in chemical engineering

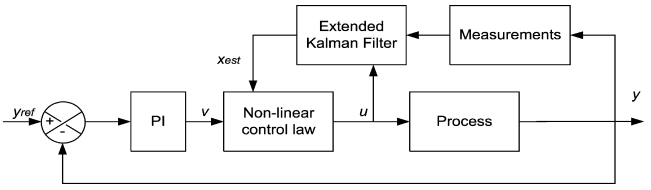

Figure 2. Nonlinear geometric control block diagram.

$$\begin{aligned} \dot{x} &= f(x) + g(x)u \\ y &= h(x) \end{aligned} \tag{33}$$

where x is the state vector, u the input vector, and y the output vector. The necessary condition for the input/output linearization is found by means of the relative degree r, which is the smallest integer such that[35]

$$L_g L_f^{\,r-1} h(x) \neq 0 \tag{34}$$

r is the number of times that the output y must be differentiated to make the input u appear linearly. The control law can be written as

$$u = \frac{v - L_f^{\,r} h(x)}{L_g L_f^{\,r-1} h(x)} \tag{35}$$

where v is an external input and $L_f^{\,i} h$ is the ith Lie derivative of the function h along the vector f. Finally, a pole placement is introduced by modifying control law (eq 35) as

$$u = \frac{v - L_f^{\,r} h(x) - \sum_{i=0}^{r-1} c_i L_f^{\,i} h(x)}{L_g L_f^{\,r-1} h(x)} \tag{36}$$

where the coefficients c_i are tuned in order to perform the desired pole placement.[32] Furthermore, an external PI controller is specified to ensure the controller robustness,[37] that is, to cope with model uncertainties, unconsidered dynamics

$$v = K_c \left[(y_{sp} - y) + \frac{1}{\tau_I} \int_0^t (y_{sp} - y)\, d\tau \right] \tag{37}$$

4.2. Extended Kalman Filter. The extended Kalman filter, an extension of the linear Kalman filter to nonlinear models, is used to estimate the states of a stochastic nonlinear dynamic system, obtained from the original deterministic nonlinear dynamic system by the addition of Gaussian state noise and measurement noise.[38] The extended Kalman filter has been applied satisfactorily in several chemical and biochemical processes.[15,32,39] Consider, the stochastic nonlinear model, continuous with respect to the states, discrete with respect to the measurements

$$\begin{aligned} \dot{x} &= f(x, u, t) + w(t) \\ y_k &= h(x(t_k), k) + v_k \end{aligned} \tag{38}$$

where w and v_k are Gaussian noises of covariance matrices Q and R for process and measurement, respectively. In this way, the predictor-corrector version of the continuous-discrete extended Kalman filter can be summarized as

Prediction Step. State estimates are obtained by integration of (eq 39) between $k-1$ and k

dx.doi.org/10.1021/ie402296j | Ind. Eng. Chem. Res. 2014, 53, 7397−7408

$$\dot{\hat{x}}^- = f(\hat{x}^-, u, t) \tag{39}$$

and similarly for the covariance matrix with equation (eq 40)

$$\dot{P}^- = FP^- + P^-F^T + Q \tag{40}$$

Correction Step. At time k, the Kalman gain is defined by

$$K_k = P_k^- H_k^T [H_k P_k^- H_k^T + R_k]^{-1} \tag{41}$$

and the corrected state estimate, also denoted a posteriori estimate, is calculated as

$$\hat{x}_k^+ = \hat{x}_k^- + K_k[y_k - h(\hat{x}_k^-)] \tag{42}$$

where y_k represents the measurements. The correction term in (eq 42) can be considered as a feedback correction of the estimated states. Finally, the updated covariance estimation is

$$P_k^+ = (I - K_k H_k) P_k^- \tag{43}$$

with

$$F = \frac{\partial f}{\partial x}|_{\hat{x}_k} \text{ and } H = \frac{\partial h}{\partial x}|_{\hat{x}_k} \tag{44}$$

5. CONTROLLER PERFORMANCE

An industrial scale reactor of a Colombian resin company (11 m^3 of capacity) is simulated where a semibatch emulsion polymerization reaction of vinyl acetate was performed. The used recipe is shown in Table 2.

Table 2. Recipe Used in the Simulations

variable	value
temperature set point (K)	351
water (kg)	5400
vinyl acetate (kg)	4651
potassium persulfate (kg)	22.8
polyvinyl alcohol (kg)	701

The controlled output is the temperature of the reactor contents. The reactor temperature set point was fixed taking into account the preheating step. As a manipulated variable, the position of a three-way valve was used, that imposes the respective flow rates through the cold and hot heat exchangers so that the inlet coolant temperature $T_{j_{in}}$ (eq30) could be also considered as the manipulated variable (Figure 1). Thus, the system is single input−single output. The monomer flow rate was fixed at a nearly constant value during approximately all the reaction time and initiator flow rate injections were programmed at specific instants during a given time.

A complete model describes in detail the reactor behavior and the polymerization reaction, including the moments of the polymer chains described in eqs 23−25. For control purposes, in order to simplify the nonlinear geometric control law and the state estimation, a reduced model is built where these three moments are not taken into account in the state vector. Thus, the state vector of the reduced model for control and estimation is $(x_1, x_2, x_3, x_4, x_5, x_6) = (I, M_t, M_M, V_{pol}, T, T_j)$. Among these states, I, M_t, and V_{pol} are not observable, they are only predicted, that is, they are obtained by simple integration of the differential equations without correction. The continuous-discrete extended Kalman filter is implemented to estimate the three states M_M, T, T_j, which are used in the nonlinear control law as will be explained later. The input and output of the observer are the same as those of the nonlinear controller. It must be noted that the estimations or predictions which are provided are useful also for monitoring of the reactor. Concerning the nonlinear control law, the relative degree of the reduced model is equal to 2. Thus, according to eq 36, the control law is

$$u = \frac{v - L_f{}^2 h(x)}{L_g L_f h(x)} \tag{45}$$

subsequently modified by the addition of the pole placement and of the PI in the external input, as

$$u = \frac{K_c\left[(y_{sp} - y) + \frac{1}{\tau_I}\int_0^t (y_{sp} - y)d\tau\right] - c_0 h(x) - c_1 L_f h(x) - L_f{}^2 h(x)}{L_g L_f h(x)} \tag{46}$$

where

$$L_f h(x) = \frac{\sum q_i C_{p,i}(T_i - \hat{T}) - \Delta H_r \mathcal{R}_{pol} + UA(\hat{T}_j - \hat{T}) - Q_{cond}}{\sum m_i C_{p,i}} \tag{47}$$

$$L_f{}^2 h(x) = -\frac{L_f h(x)}{\sum m_i C_{p,i}}\left[M_{wM} C_{ppol} q_M + M_{wM} C_{pM}(q_M - \mathcal{R}_{pol}) + \sum q_i C_{p,i} + \Delta H_r \mathcal{R}_{pol} k_p\left(\frac{6.310^3}{R\hat{T}^2}\right) + UA\right] + UA\left[\frac{F_j(T_{cold} - \hat{T}_j)}{m_w} - \frac{UA}{m_w C_{p,water}}(\hat{T}_j - \hat{T})\right] \tag{48}$$

$$L_g L_f h(x) = UA\frac{F_j(T_{hot} - T_{cold})}{m_w} \tag{49}$$

It can be observed that the control law uses the states estimated by the Kalman filter ($\hat{M}_M$, $\hat{T}$, and $\hat{T}_j$). The term $\mathcal{R}_{pol}$ is calculated from the derivative of $\hat{M}_M$. In particular, it should be noticed that the term $\sum m_i C_{p,i}$ represents the summation of all the heat capacities contained in the reactor as

$$\sum m_i C_{p,i} = \hat{M}_M M_{wM} C_{pM} + (\hat{M}_t - \hat{M}_M) M_{wM} C_{ppol} + \rho_w V_w^w C_{p,water} + m_{PVOH} C_{pPVOH} \tag{50}$$

and, therefore $\hat{M}_M$, $\hat{T}$, and $\hat{T}_j$ influence the control law.

The control law parameters $\{c_i, K_c, \tau_I\}$ are determined by means of a pole placement[32] using minimization of the ITAE criterion to obtain the desired stability characteristics from the closed loop transfer function equal to

$$\frac{Y(s)}{Y_{sp}(s)} = \frac{K_c\left(s + \frac{1}{\tau_I}\right)}{s^3 + c_1 s^2 + (c_0 + K_c)s + \frac{K_c}{\tau_I}} \tag{51}$$

With respect to the extended Kalman filter calculations, the reactor temperature is the only measurable state variable with a sampling period equal to 20s.

In this section, results for the nominal case studied are presented. Then, some additional simulations are made in order to test the robustness of the controller and of the state estimator.

dx.doi.org/10.1021/ie402296j | Ind. Eng. Chem. Res. 2014, 53, 7397−7408

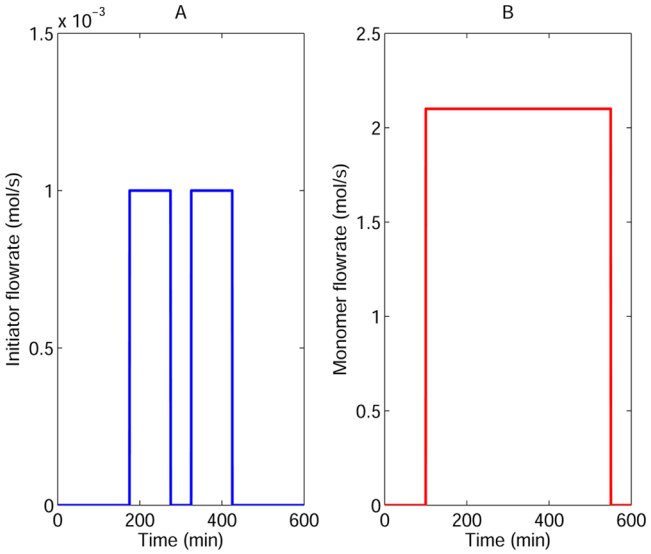

Figure 3. Feed policies for reactants: (A) Initiator molar flow rate and (B) monomer molar flow rate.

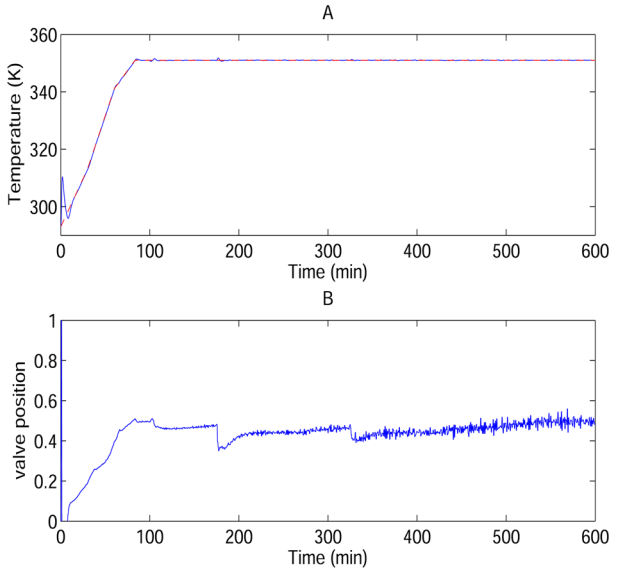

Figure 4. Temperature control for the nominal case. (A) Controlled variable: Reactor temperature (blue line) and temperature set point (red line). (B) Manipulated variable: position of the three-way valve.

5.1. Nominal Case. Two injections of initiator were included (Figure 3A) in the nominal case where the set point is equal to 351 K. The injections can be considered disturbances to the system taking into account their influence on the temperature. Figure 4 shows the closed loop profiles of the reactor temperature and valve position. Nonlinear geometric control presents a good performance, first tracking the rising set point, then following the constant set point and rapidly rejecting the disturbances caused by initiator injections. Figure 5 shows the molecular polymer properties. It can be observed that the dispersity of the polymer tends to be 2 while, at the same time, monomer conversion is approximately 95%. It seems that the monomer conversion could be improved by increasing the initiator flow rate or the temperature. These alternatives will be explored after verifying the controller performance. Initiator injections influence the heating power released by the reacting system to be removed by the reactor jacket. In Figure Figure 6, the heating power produced during the whole batch is shown. The two highest peaks of 320 and 250 kW at instants 175 and 325 min, respectively, are due to the two injections of initiator. The first peak around of 60 min corresponds to the effect of the initial amount of initiator charged to the reactor which starts to react at that time when the temperature has increased sufficiently to activate the reaction. The most interesting point to notice is that the nonlinear controller reacts promptly (Figure 4) and the temperature profile is maintained nearly constant in spite of the strong disturbances introduced by initiator injections.

5.2. Robustness Study. Robustness tests about the control law using the extended Kalman filter estimations were performed by introducing systematic errors in the reduced model. The goal is to verify the controller performance under significant changes made in the reduced model used for the calculation of the control law whereas the model of the plant is left unchanged.

5.2.1. Activation Energy Error. First, it will be assumed that the activation energy E_a of the propagation reaction is increased by 10% with respect to its real value. The temperature reactor, which is the only measured variable, is estimated without noticeable error (Figure 7A) whereas the monomer conversion (Figure 7B) displays a deviation due to the model error.

A similar behavior could be observed, for example by decreasing by 50% the propagation rate constant k_p calculation. These two parameters are crucial in the dynamic thermal response of the system and therefore their influence on the temperature control loop performance is strong.

5.2.2. Heat Transfer Coefficient Error. In the second robustness test, representative of the real industrial situation, it will be assumed that the heat transfer coefficient U is decreased in a 20% with respect to its real value. The operating conditions can change due to equipment fouling and variations in the properties like viscosity and solids content also affect the value of U. In consequence, by means of this reduction of U, we are assuming that initially there is an important effect of fouling and it is stronger at the end of the batch when the viscosity and solids content are higher than at the beginning. In the process model, it was mentioned that the heat transfer coefficient is calculated taking into account the effect of the solids content according to eq 32 in such a way that U is not constant.

Figure 8 shows that, in the first 300 min, there is not an important difference between the estimated monomer conversion and the real value, in spite of the assumption of 20% of reduction of U. In the last part of the batch, the solids content and viscosity increase importantly (Figure 9), modifying heat and mass transfer mechanisms, which explains the poor estimation of the monomer conversion. However, a good temperature control is achieved demonstrating the work of nonlinear control and its robustness. Similar results to those of Figure 8 are obtained by reducing U at the beginning of the reaction and after maintaining this value constant during all the batch. Again, the most important effects are observed during the last interval of the reaction.

5.3. Set Point Tracking. To test the tracking performance of the nonlinear geometric controller, a set point change of temperature was made from 351 to 356K during a period of 85 min (Figure 10A). Again, the controller works well following the variable set point while rejecting the initiator injection disturbances. Of course, the manipulated input shows more important transients (Figure 10B) about the set point change instants than in the previous cases of regulation. These aggressive actions

dx.doi.org/10.1021/ie402296j | Ind. Eng. Chem. Res. 2014, 53, 7397−7408

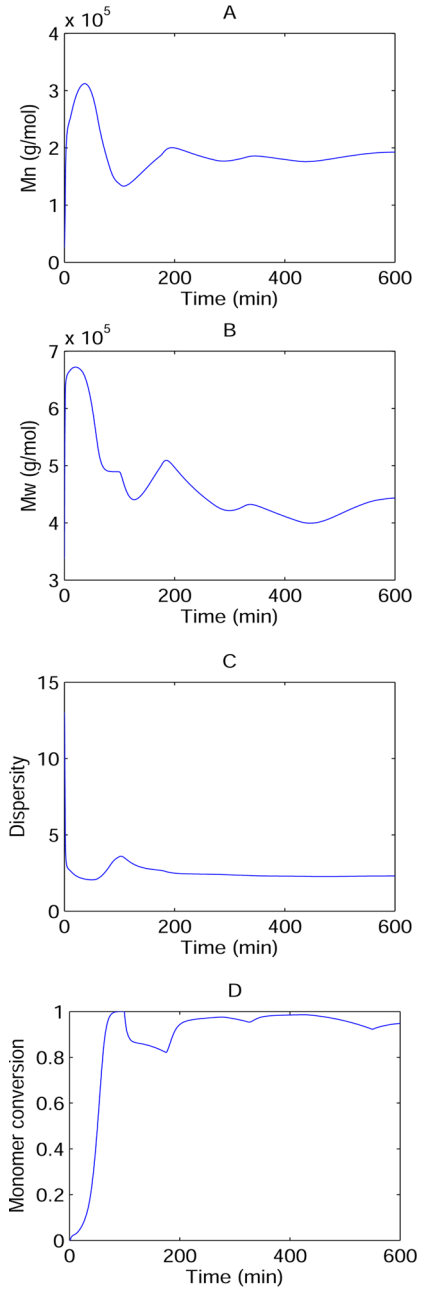

Figure 5. Polymer properties profile for the nominal case: (A) Number average molecular weight, (B) weight average molecular weight, (C) dispersity, and (D) monomer conversion.

aim at following the new temperature set point quickly with limited overshoot. The overshoot prevention is important for the process because a larger temperature overshoot could cause an important increase in reaction kinetics and a gel effect as a consequence.

5.4. Comparison with a Digital PID Controller. In regulatory control, the PID feedback controller is the most traditional and widely used technique, it is easily implemented, a mathematical model of the process is not required and therefore, a minimum process knowledge is required for its design. However, this technique presents drawbacks mainly due to measurement delays, process non linearities and delays, process disturbances, interactions between process variables, absence of output prediction on a large horizon opposite to

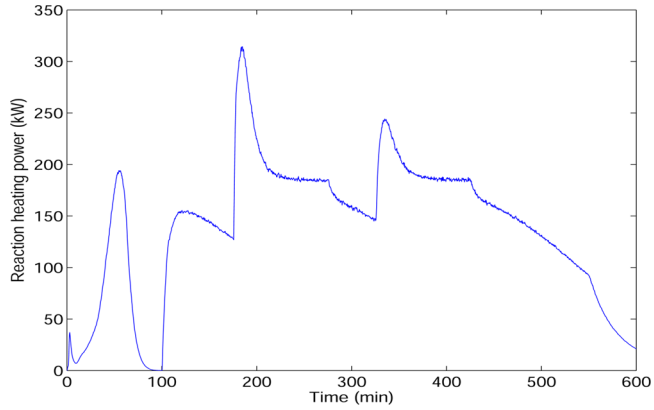

Figure 6. Reaction heating power produced in the nominal case.

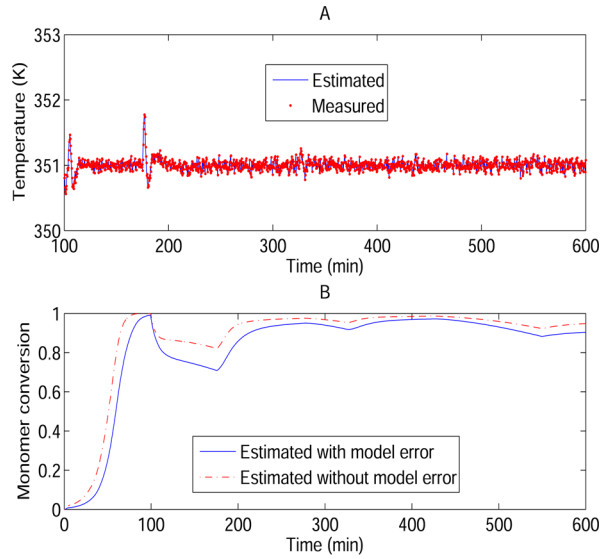

Figure 7. Results for a 10% error of activation energy: (A) Reactor temperature (set point = 351 K) and (B) monomer conversion.

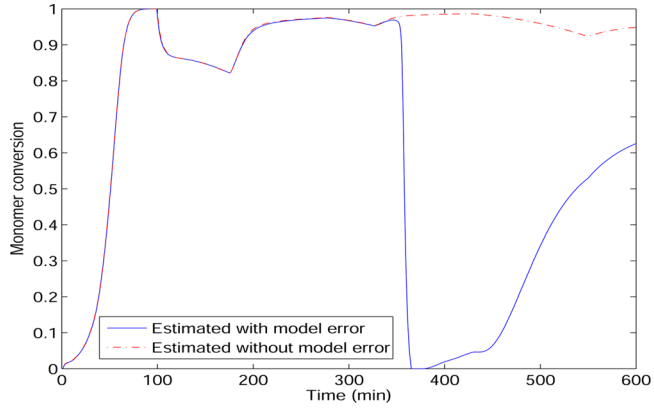

Figure 8. Monomer conversion estimation with heat transfer coefficient error.

model predictive control. Here, to compare the performance of a conventional controller with the nonlinear controller, the control law of a digital PID control is implemented and tested for a case in which three initiator injections (As will be discussed in the next section) are used, as can be noticed in Figure 12. The results of PID control are shown in Figure 11 and the corresponding performance of the nonlinear controller is

dx.doi.org/10.1021/ie402296j | Ind. Eng. Chem. Res. 2014, 53, 7397−7408

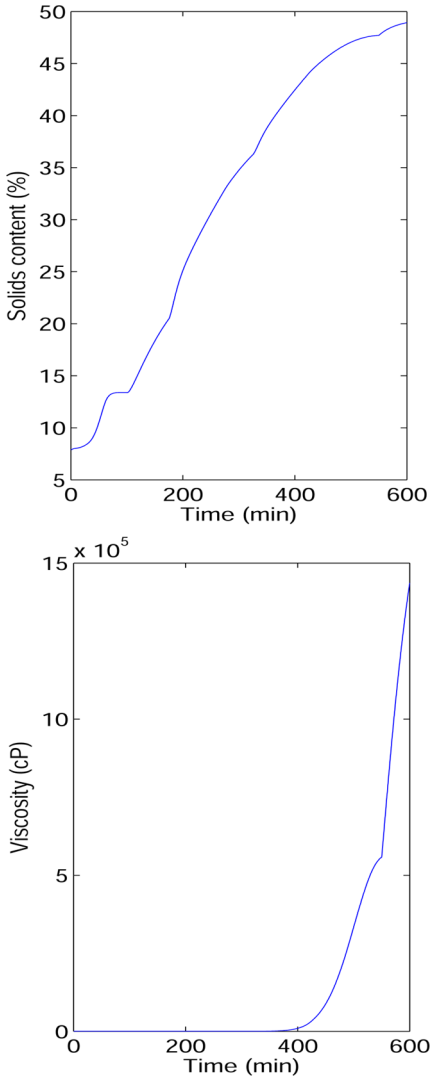

Figure 9. Solids content and viscosity of the reacting mixture with heat transfer coefficient error.

presented in Figure 13. It is clear that the PID controller is not able to follow the constant set point of 351 K imposed to reactor temperature during all the batch. In particular, when the initiator is injected, the temperature deviates significantly increasing up to 365 K for the first initiator injection, 360 K for the second injection, and 363 K for the last initiator injection, thus resulting in overshoots by more than 10K. These peaks are typical from PID control and, in the case of emulsion polymerization, it has been reported recently[13] that this limits the values of the possible initiator flow rates fed to the reactor and it increases the batch time in order to reduce temperature oscillations and peaks and to obtain the desired polymer properties.

6. PROCESS IMPROVEMENT

In the previous section, it was demonstrated that nonlinear geometric control offers a good performance in controlling the emulsion polymerization process. Now, some improvement options will be explored taking advantage of the previously designed controller. Initially, as mentioned before, monomer conversion will be improved by increasing the total quantity of initiator added to the reactor. To do this, a simulation using three initiator injections instead of two was made as shown in

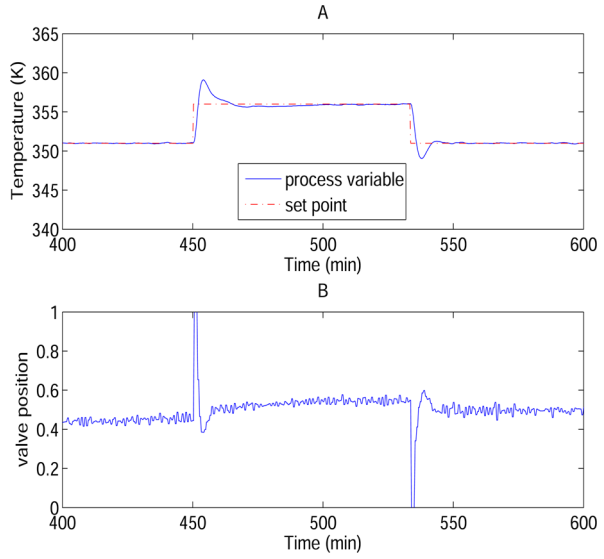

Figure 10. Set point tracking: (A) Temperature profile with set point and (B) Manipulated variable.

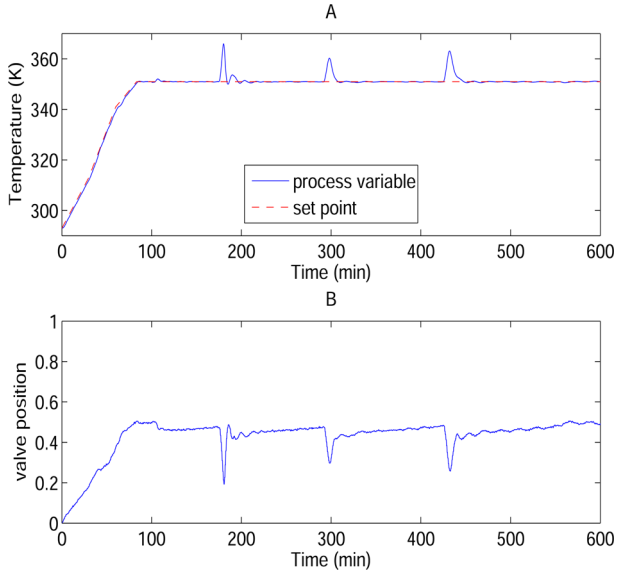

Figure 11. PID regulation: (A) Temperature profile with set point and (B) Manipulated variable.

Figure 12. The total quantity of initiator fed (12 mol) is maintained constant here by using three injections of 4 mol (2×10^{-3} mol/s for 2000 s) each instead of two injections of 6 mol (1×10^{-3} mol/s for 6000 s) each one. Results of the temperature profile are shown in Figure Figure 13A. With three injections (i.e., one additional disturbance during the batch), the controller still works well and the monomer conversion is increased from 95% to 98.6% whereas the solids content also increases from 48.5% to 50.7%. The power released by the reacting system (approximately 400 kW) shows peaks similar to Figure Figure 13C, which are managed without problem by heat transfer through the jacket by means of the efficient nonlinear temperature controller. In this way, it is demonstrated that, in a first approach, the polymer quality and monomer conversion can be improved. The potential of nonlinear control to manage the number and quantities of initiator injections, opening the possibility of optimizing the initiator feed to the

dx.doi.org/10.1021/ie402296j | Ind. Eng. Chem. Res. 2014, 53, 7397−7408

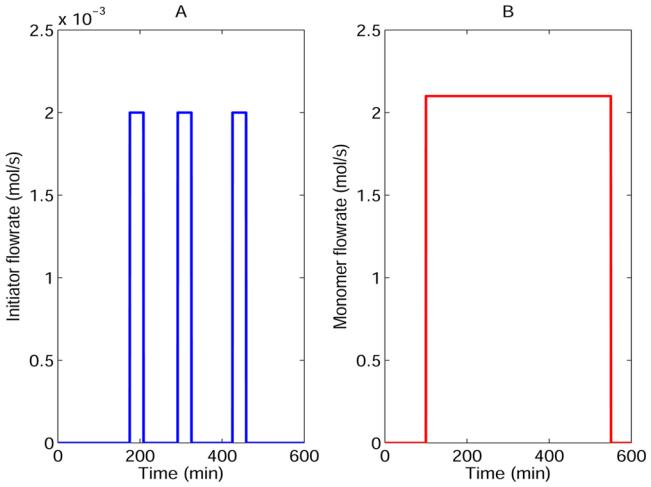

Figure 12. Increase of feed policies for initiator: (A) Initiator molar flow rate and (B) monomer molar flow rate.

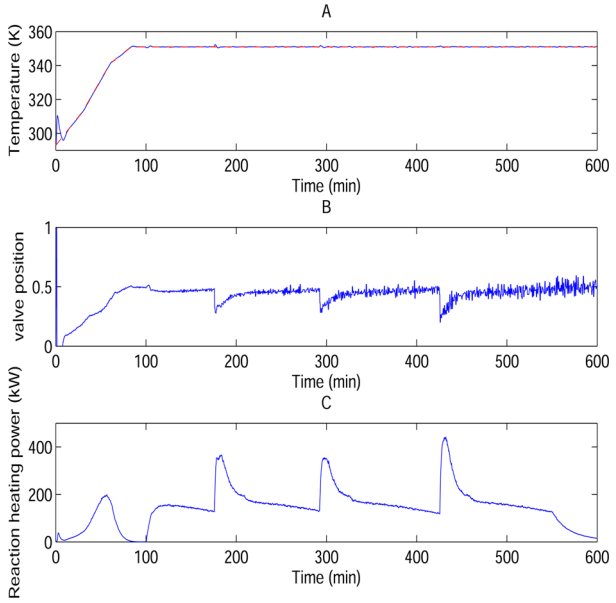

Figure 13. Results for three initiator injections: (A) Temperature profile with set point, (B) manipulated variable, and (C) reaction heating power released.

process, is also verified. A second possibility to manage initiator injection is to redistribute it in a different way into the whole batch in order to have a smoother feeding and, in consequence, a better temperature control and stability of the reaction. To do this, we have taken a constant initiator flow rate of 10^{-3} mol/s injected during a period of time representative of the major part of the batch (400 min). The results are shown in Figures Figure 14 and Figure 15. The solids content increases up to 51% while the viscosity reaches 6.3×10^6 cP. Four important facts can be observed: (1) The control action is smoother than when discrete impulses of initiator injections are performed (Figure 14A, B). (2) Quality results reported in Figure 15 are higher with regard to monomer conversion and solids content for the same quantity of monomer added. In this way, it is possible to increase the solids content or to consider the possibility of decreasing the batch time to achieve a standardized value of some polymer properties. (3) Polymer dispersity tends to be close to 2 (Figure 15), ensuring higher homogeneity than

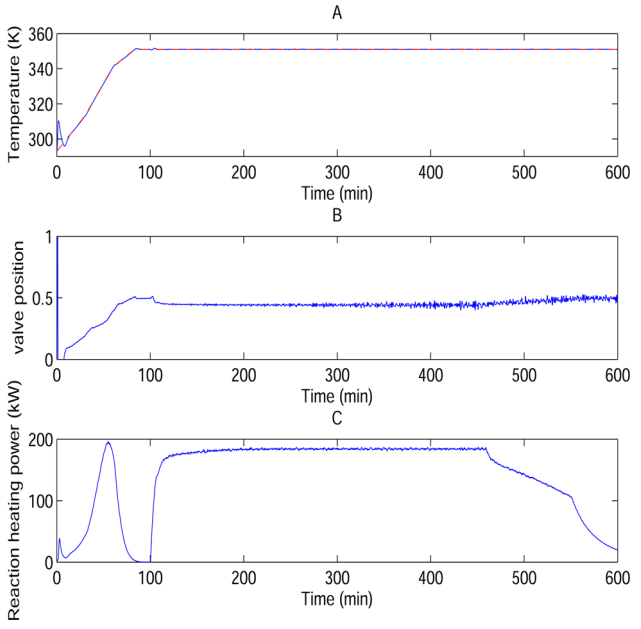

Figure 14. Results for a constant initiator injection: (A) Temperature profile with set point, (B) manipulated variable, and (C) reaction heating power released.

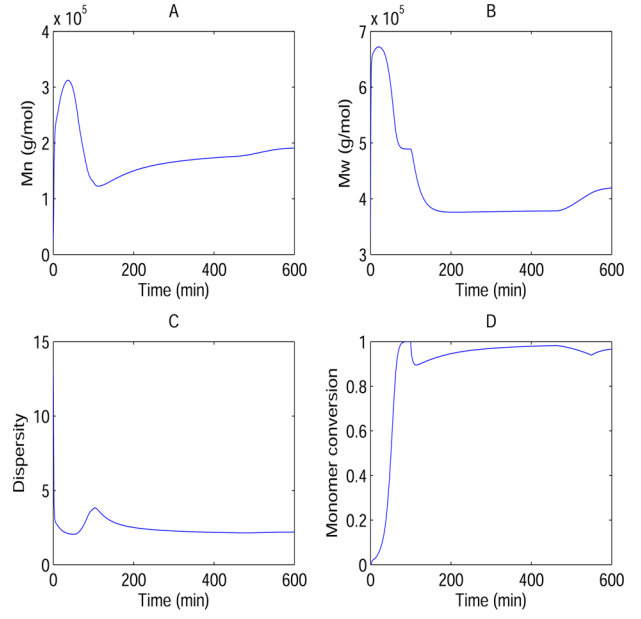

Figure 15. Polymer properties profile for one initiator injection: A. Number average molecular weight, B. Weight average molecular weight, C. Dispersity, D. Monomer conversion.

in the case of several initiator injections. (4) The heat of polymerization is better distributed into the whole batch. There are no peaks of power released (Figure 14C) and, in this way, a safer operation is guaranteed.

In general terms, one constant injection of initiator can be managed by the nonlinear geometric controller and this is beneficial for the stability of the reaction and the final polymer properties whereas safe operation is also guaranteed. Clearly, limitations encountered with PID control are not reported in the case of nonlinear control and this is a good starting point to test new operating strategies, mainly related to feeds to the reacting system and their influence over the final polymer

dx.doi.org/10.1021/ie402296j | Ind. Eng. Chem. Res. 2014, 53, 7397−7408

properties. It is important to note that dynamic optimization could be performed in order to obtain optimal initiator feed policies in combination with a temperature profile which allows us to achieve desired properties and reduce batch time under safety operating conditions.

7. CONCLUSION

Emulsion polymerization is an industrially important process characterized by strong nonlinearities and large exothermicity that creates difficulties in temperature control and causes undesired polymer quality variations. For this reason, in this work, initially a model of an industrial emulsion polymerization reactor is built to correctly represent the main molecular characteristics of the polymer and the reactor behavior. The model allows us to estimate the effect of initiator and monomer dosing as well as the influence of temperature on the reaction. A nonlinear controller is designed in order to track the temperature in the reacting system in spite of typical disturbances such initiator and monomer injections. An extended Kalman filter is used to estimate the states and is tested in different cases including a robustness study where model errors are introduced. Finally, after verification of controller performance, some process changes were proposed in order to improve process productivity and polymer quality. Future work will be done by calculating the optimal temperature profile or optimal feed policy of the monomer and initiator in a dynamic optimization study that can be used to provide the optimal set points for future nonlinear control. It would also be interesting to compare the performance and robustness of model predictive control to present nonlinear control.

■ ASSOCIATED CONTENT

Supporting Information

This material is available free of charge via the Internet at http://pubs.acs.org.

■ AUTHOR INFORMATION

Corresponding Author

*E-mail: jean-pierre.corriou@univ-lorraine.fr. Phone: +33 (0) 383175213. Fax: +33 (0)383175326.

Notes

The authors declare no competing financial interest.

■ ACKNOWLEDGMENTS

The authors thank the financial support of the Embassy of France, Colfuturo and Universidad Nacional de Colombia.

■ NOMENCLATURE

C_{pj} = specific heat of component j [J K^{-1} kg^{-1}]
I = moles of initiator in the reactor [mol]
k_a = rate coefficient for radical entry [m^3 mol^{-1} s^{-1}]
k_{fm} = rate constant for chain transfer to monomer [m^3 mol^{-1} s^{-1}]
k_{fp} = rate constant for chain transfer to polymer [m^3 mol^{-1} s^{-1}]
k_p = propagation rate constant [m^3 mol^{-1} s^{-1}]
k_t = termination rate constant [m^3 mol^{-1} s^{-1}]
k_I = overall initiation rate constant [s^{-1}]
K_M^p = phase distribution coefficient of monomer between particle and water phases
K_M^d = phase distribution coefficient of monomer between droplet and water phases
M_M = moles of monomer in the reactor [mol]
M_t = total moles of monomer fed to the reactor [mol]
M_{wM} = monomer molecular weight [kg mol^{-1}]
m_w = mass of water in the reactor jacket [kg]
$[M]^p$ = monomer concentration in the particle phase [mol m^{-3}]
$[M]^w$ = monomer concentration in the water phase [mol m^{-3}]
$\bar{M}_n$ = number average molecular weight [kg mol^{-1}]
$\bar{M}_w$ = weight average molecular weight [kg mol^{-1}]
$\bar{n}$ = average number of radicals per particle
N_A = Avogadro's number
N_p = number of particles
q_I = Flow rate of initiator fed to the reactor [mol s^{-1}]
q_M = Flow rate of monomer fed to the reactor [mol s^{-1}]
$\mathcal{R}_{pol}$ = overall reaction rate [mol s^{-1}]
$\mathcal{R}_{pol}^p$ = propagation rate in the polymer phase [mol s^{-1}]
$\mathcal{R}_{pol}^w$ = propagation rate in the aqueous phase [mol s^{-1}]
$[R]^w$ = Overall concentration of radicals in the water phase [mol.m^{-3}]
T = reactor temperature [K]
T_j = jacket temperature [K]
U = overall heat transfer coefficient [W m^{-2} K^{-1}]
V_{pol} = total volume of polymer generated in the reaction [m^3]
V^i = total volume of phase i [m^3]
V_j^i = volume of component j in phase i [m^3]
z = adjustable parameter
α = probability of propagation
ΔH_r = heat of reaction [J kg^{-1}]
λ_0 = total concentration of zeroth moment for growing chains
μ_0 = concentration of zeroth moment for dead chains
μ_1 = concentration of first moment for dead chains
μ_2 = concentration of second moment for dead chains
ϕ_S = solids content
ρ_M = monomer density [kg m^{-3}]
ρ_{pol} = polymer density [kg m^{-3}]

Nomenclature for control

x state vector
u input vector
y output
r relative degree
$L_f^i h$ ith Lie derivative of the function h
K Kalman filter gain
$\hat{x}$ state estimate
v external input

■ REFERENCES

(1) Odian, G. *Principles of Polymerization*; Wiley Interscience, John Wiley & Sons: Hoboken, NJ, 2004.
(2) Yildirim, H. *Vinyl Acetate Emulsion Polymerization and Copolymerization with Acrylic Monomers*; CRC Press: Boca Raton, FL, 2000.
(3) Penlidis, A.; MacGregor, J. F.; Hamielec, A. E. Dynamic modeling of emulsion polymerization reactors. *AIChE J.* **1985**, *31*, 881−889.
(4) Dimitratos, J.; Eliçabe, G.; Georgakis, C. Control of emulsion polymerization reactors. *AIChE J.* **1994**, *40*, 1993−2021.
(5) Zeaiter, J.; Romagnoli, J. A.; Gomes, V. G. Online control of molar mass and particle-size distributions in emulsion polymerization. *AIChE J.* **2006**, *52*, 1770−1779.
(6) Srour, M. H.; Gomes, V. G.; Altarawneh, I. S.; Romagnoli, J. A. Online model-based control of an emulsion terpolymerization process. *Chem. Eng. Sci.* **2009**, *64*, 2076−2087.
(7) Ray, W. H. Polymerization reactor control. *IEEE Control Syst. Mag.* **1986**, 3−8.

(8) Sheibat-Othman, N.; Othman, S.; Boyron, O.; Alamir, M. Multivariable control of the polymer molecular weight in emulsion polymerization processes. *J. Process Control* **2011**, *21*, 861−873.
(9) Eliçabe, G. E.; Meira, G. R. Estimation and control in polymerization reactors. *Polym. Eng. Sci.* **1988**, *28*, 121−135.
(10) Soroush, M. State and parameter estimations and their applications in process control. *Comp. Chem. Eng.* **1998**, *23*, 229−245.
(11) Richards, J. R.; Congalidis, J. P. Measurement and control of polymerization reactors. *Comp. Chem. Eng.* **2006**, *30*, 1447−1463.
(12) Arora, S.; Gesthuisen, R.; Engell, S. Model based operation of emulsion polymerization reactors with evaporative cooling: Application to vinyl acetate homopolymerization. *Comp. Chem. Eng.* **2007**, *31*, 552−564.
(13) Hvala, N.; Aller, F.; Miteva, T.; Kukanja, D. Modelling, simulation and control of an industrial, semi-batch, emulsion-polymerization reactor. *Comp. Chem. Engng* **2011**, *35*, 2066−2080.
(14) Wang, Z. L.; Pla, F.; Corriou, J. P. Nonlinear adaptive control of batch styrene polymerization. *Chem. Eng. Sci.* **1995**, *50*, 2081−2091.
(15) Sheibat-Othman, N.; Othman, S. Control of an emulsion polymerization reactor. *Ind. Eng. Chem. Res.* **2006**, *45*, 206−211.
(16) Corriou, J. P. Multivariable control of an industrial gas phase copolymerization reactor. *Chem. Eng. Sci.* **2007**, *62*, 4903−4909.
(17) Gentric, C.; Pla, F.; Latifi, M. A.; Corriou, J. Optimization and non-linear control of a batch emulsion polymerization reactor. *Chem. Eng. J.* **1999**, *75*, 31−46.
(18) Thickett, S. C.; Gilbert, R. G. Emulsion polymerization: State of the art in kinetics and mechanisms. *Polymer* **2007**, *48*, 6965−6991.
(19) Birtwistle, D. T.; Blackley, D. C. Theory of compartmentalised free-radical polymerisation reactions Part 4. *J. Chem. Soc., Faraday Trans. I* **1981**, *77*, 413−426.
(20) Birtwistle, D. T.; Blackley, D. C. Theory of compartmentalised free-radical polymerisation reactions Part 5. *J. Chem. Soc., Faraday Trans. I* **1981**, *77*, 1351−1358.
(21) Brooks, B. W. Simplifications in the kinetic schemes for emulsion polymerisation. *J. Chem. Soc., Faraday Trans. I* **1982**, *78*, 3137−3143.
(22) O'toole, J. T. Kinetics of emulsion polymerization. *J. Appl. Polym. Sci.* **1965**, *9*, 1291−1297.
(23) Stockmayer, W. H. Note on the kinetics of emulsion polymerization. *J. Polym. Sci.* **1957**, *24*, 314−317.
(24) Li, B.; Brooks, B. W. Prediction of the average number of radicals per particle for emulsion polymerization. *J. Polym. Sci., Part A: Polym. Chem.* **1993**, *31*, 2397−2402.
(25) Sáenz de Buruaga, I.; Echevarría, A.; Armitage, P. D.; de la Cal, J. C.; Leiza, J. R.; Asua, J. On-line control of a semibatch emulsion polymerization reactor based on calorimetry. *AIChE J.* **1997**, *43*, 1069−1081.
(26) Vicente, M.; Leiza, J. R.; Asua, J. M. Maximizing production and polymer quality (MWD and composition) in emulsion polymerization reactors with limited capacity of heat removal. *Chem. Eng. Sci.* **2003**, *58*, 215−222.
(27) McKenna, T. F.; Graillat, C.; Guillot, J. Contributions to defining the rate constants for the homo- and copolymerisation of butyl acrylate and vinyl acetate. *Polym. Bull.* **1995**, *34*, 361−368.
(28) Penlidis, A. Polymer reactor design, optimization and control in latex production technology. PhD thesis, McMaster University, Hamilton, Ontario, 1986.
(29) Araújo, P.; Giudici, R. Optimization of semicontinuous emulsion polymerization reactions by IDP procedure with variable time intervals. *Comp. Chem. Eng.* **2003**, *27*, 1345−1360.
(30) Chatterjee, A.; Park, W. S.; Graessley, W. W. Free radical polymerization with long chain branching: continuous polymerization of vinyl acetate in *t*-butanol. *Chem. Eng. Sci.* **1977**, *32*, 167−178.
(31) Bindlish, R.; Rawlings, J. Target linearization and model predictive control of polymerization processes. *AIChE J.* **2003**, *49*, 2885−2899.
(32) Corriou, J. P. *Process Control—Theory and Applications*; Springer Verlag: London, England, 2004.
(33) Kravaris, C.; Kantor, J. C. Geometric methods for nonlinear process control. 1. Background. *Ind. Eng. Chem. Res.* **1990**, *29*, 2295−2310.
(34) Kravaris, C.; Kantor, J. C. Geometric methods for nonlinear process control. 2. Controller synthesis. *Ind. Eng. Chem. Res.* **1990**, *29*, 2310−2323.
(35) Isidori, A. *Nonlinear Control Systems*, 3rd ed.; Springer-Verlag: New York, 1995.
(36) Khalil, H. K. *Nonlinear Systems*; Prentice Hall: Upper Saddle River, NJ, 1996.
(37) Palanki, S.; Kravaris, C. Controller synthesis for time-varying systems by input/ouput linearization. *Comp. Chem. Eng.* **1997**, *21*, 891−903.
(38) Simon, D. *Optimal State Estimation: Kalman, H∞, and Nonlinear Approaches*; Wiley Interscience, John Wiley & Sons: Hoboken, NJ, 2006.
(39) Dochain, D. State and parameter estimation in chemical and biochemical processes: A tutorial. *J. Process Control* **2003**, *13*, 801−818.